Isoscalar Meson Exchange Currents and the Deuteron Form Factors

Hiroshi Ito
Center for Nuclear Studies, Department of Physics, George Washington University, Washington, D.C. 20052

Franz Gross
Physics Department, College of William and Mary, Williamsburg, Virginia 23185
and Continuous Electron Beam Accelerator Facility, 12000 Jefferson Avenue, Newport News, Virginia 23606

(Received 11 June 1993)

Electromagnetic form factors for the $\rho\pi\gamma$ and $\omega\sigma\gamma$ vertices, estimated from quark loop diagrams, differ considerably from the monopole form factors obtained from vector meson dominance, and significantly alter the predictions for the elastic electromagnetic form factors of the deuteron.

PACS numbers: 25.30.Bf, 13.40.Fn, 24.85.+p, 27.10.+h

A number of experimental measurements, the most famous being the electrodisintegration of the deuteron at threshold, have established the existence of *isovector* meson exchange currents [1]. In contrast, the nature and size of *isoscalar* exchange currents are still issues of some controversy. The $\rho\pi\gamma$ interaction (related to the AVV anomaly [2]) certainly leads to an isoscalar exchange current, but because of the large mass and width of the ρ and the comparatively small size of the $\rho\pi\gamma$ coupling, such a current is hard to distinguish from other short range interaction currents, including those which might arise from quark exchange forces [3]. Use of the $\omega\sigma\gamma$ isoscalar exchange interaction is more dubious. Both the very short range nature of this current and the phenomenological status of the σ make it hard to justify, singling it out for special consideration.

The simplest system in which to look for isoscalar exchange currents is the deuteron. The deuteron structure functions $A(Q^2)$ and $B(Q^2)$ have been calculated using a variety of relativistic schemes for treating the nuclear dynamics [4–8], and good deuteron wave functions can be derived from realistic models of the NN interaction based on meson field theory [9, 10]. The relativistic theory for electron-deuteron elastic scattering is therefore fairly reliable. In the context of a Bethe-Salpeter one boson exchange (OBE) model of the nuclear force, the form factors can be calculated from only two contributions: the relativistic impulse approximation (RIA) in which the photon couples directly to one of the bound nucleons [shown in Fig. 1 (a)], and the meson exchange current (MEC) contribution in which the photon couples to the exchanged mesons [shown in Fig. 1(b)]. Because the deuteron is an isospin zero target, only the isoscalar MEC can contribute, and in the context of the OBE model the $\rho\pi\gamma$ and $\omega\sigma\gamma$ currents are two likely candidates.

The $\rho\pi\gamma$ and $\omega\sigma\gamma$ exchange currents make small contributions to the magnetic and quadrupole moments (which are the values of the magnetic and quadrupole form factors at $Q^2 = 0$, where Q^2 is the square of the four-momentum transferred by the photon), but these contributions are much less than $\frac{1}{2}\%$ [11]. They are therefore masked by the significantly larger (and uncertain) relativistic corrections, which are about 5% for the magnetic moment and 1.5% for the quadrupole moment [9]. The situation is more favorable at large Q^2, where these MEC contributions are expected to be large (because they provide a mechanism for sharing the incoming photon momentum equally between the two nucleons) [12–14], and where previous calculations of the RIA [4, 5, 11] have underestimated $A(Q^2)$ by an order of magnitude at $Q^2 = 4$ GeV$^2/c^2$ and have also failed to predict the correct location for the dip in $B(Q^2)$, as shown by the solid lines in Fig. 2. Recently Hummel and Tjon [11] used these isoscalar exchange currents to resolve this discrepancy at high Q^2. However, the size of these MEC depends critically on the Q^2 dependence of the form factors associated with the $\rho\pi\gamma$ and $\omega\sigma\gamma$ vertices; if no form factors are used (for example) the result from the $\rho\pi\gamma$ exchange

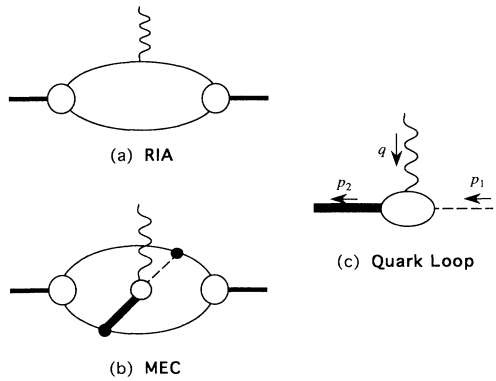

FIG. 1. (a) The relativistic impulse approximation (RIA). (b) The $\rho\pi\gamma$ (or $\omega\sigma\gamma$) meson exchange current (MEC) contribution. The ρ (or ω) is denoted by the wide shaded line and the π (or σ) by the dashed line. (c) The quark loop (QL) contribution to the $\rho\pi\gamma$ (or $\omega\sigma\gamma$) vertex, represented by the lightly shaded circle in (b).

0031-9007/93/71(16)/2555(4)$06.00

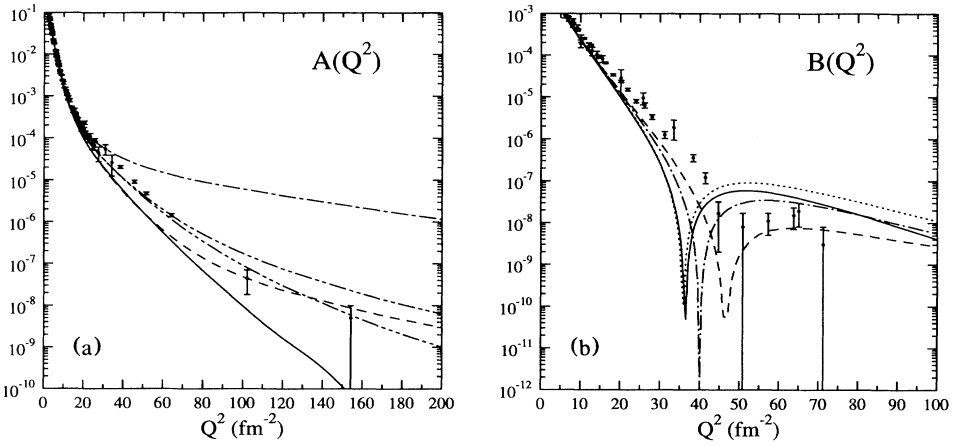

FIG. 2. Calculations of the A and B structure functions under various assumptions. In both figures the solid line is the RIA and the dashed line is the full calculation (including $\rho\pi\gamma$ and $\omega\sigma\gamma$ exchange currents with VDM form factors) of Hummel and Tjon. In (a) the lines with *one, two, or three* short dashes are the RIA plus $\rho\pi\gamma$ exchange current with *no form factor*, the VDM form factor, or the QL form factor at the $\rho\pi\gamma$ vertex, respectively. (Addition of the $\omega\sigma\gamma$ exchange current with a QL form factor has a negligible effect.) In (b) the dotted line is the RIA plus the $\rho\pi\gamma$ exchange current (with a QL form factor) and the dot-dashed line is the RIA plus *both* the $\rho\pi\gamma$ and $\omega\sigma\gamma$ exchange currents (with QL form factors).

current alone would overestimate $A(Q^2)$ by 2 orders of magnitude [Fig. 2(a)]. Therefore we must have a reliable estimate of the Q^2 dependence of the form factors at the $\rho\pi\gamma$ and $\omega\sigma\gamma$ vertices, and such an estimate should take into account the composite nature of the π, σ, ρ, and ω mesons. In this Letter we calculate these form factors from quark loop diagrams which include the $q\bar{q}$ composite structure of the π, σ, ρ, and ω mesons, and discuss the implications of our results for the MEC contributions to the deuteron structure functions.

To calculate the form factor at the $\rho\pi\gamma$ vertex we use a relativistic quark model of the pion and the rho which was previously used to calculate a variety of pion observables [15]. In this model the Bethe-Salpeter vertex function for the pion is taken to be $\Gamma_\pi(k,p) = \mathcal{N}_\pi\gamma^5\chi_f\chi_c D_S^{-1}(k^2)$, where k and p are the relative and total four-momenta of the $q\bar{q}$ pair which couple to the pion, $D_S(k^2) = k^2 - \Lambda^2$ (with Λ an adjustable parameter) is a parametrization of the momentum distribution of the $q\bar{q}$ pair, $\mathcal{N}_\pi$ is a normalization constant, and χ_c and χ_f are color and flavor wave functions. In Ref. [15] the form factor and low-energy observables of the pion were very well reproduced by choosing the quark mass $m_q = 248$ MeV and $\Lambda = 450$ MeV, and the model also successfully described the Q^2 dependence of the form factor for the $\gamma^* + \pi^0 \to \gamma$ process [16]. The ρ meson vertex was taken to be $\Gamma^\nu_\rho(k,p) = \mathcal{N}_\rho G^\nu(p)\chi_f\chi_c D_V^{-1}(k^2)$, where $G^\nu(p) = \gamma^\nu - \not{p}p^\nu/p^2$, and the normalization constant, $\mathcal{N}_\rho$, is calculated from the residue of the $q\bar{q}$ scattering amplitude in the vector channel [15]. A dipole momentum distribution $D_V(k^2) = (k^2 - \Lambda_1^2)(k^2 - \Lambda_2^2) \sim k^4$ was chosen in order to insure that the integrals involve the rho converge. Using the same quark mass, the choice $\Lambda_1 \sim 600$ MeV and $\Lambda_2 \sim 1000$ MeV fits the empirical values of the $\gamma\rho$ coupling and the rho width. In the present calculation, in order to avoid threshold singularities, we found it convenient to use a larger quark mass of $m_q \simeq 390$ MeV $> m_\rho/2$. Using this larger quark mass changes the fitted observables by only about 25%, which is sufficiently close for our estimates.

Now we use this model to calculate the $\rho\pi\gamma$ vertex, which is defined by [13]

$$\langle\rho(p_2)|J^\mu|\pi(p_1)\rangle = -i\frac{e}{m_\rho}g_{\rho\pi\gamma}f_{\rho\pi\gamma}(Q^2)\epsilon^{\mu\nu\alpha\beta}p_{1\alpha}q_\beta\epsilon_\nu\ , \tag{1}$$

where the antisymmetric tensor $\epsilon^{\mu\nu\alpha\beta}$ assures electromagnetic gauge invariance, q ($q^2 = -Q^2$) is the four-momentum of the virtual photon, ϵ_ν is the polarization vector of the ρ meson, $f_{\rho\pi\gamma}(Q^2)$ is normalized to unity at $Q^2 = 0$, and $g_{\rho\pi\gamma}$ is the coupling constant. We calculated this vertex from the quark loop diagram shown in Fig. 1(c), which gives

$$\langle\rho(p_2)|J^\mu|\pi(p_1)\rangle = e_q\int\frac{d^4k}{(2\pi)^4}\mathrm{Tr}\Big\{\ \epsilon_\nu\overline{\Gamma}^\nu_\rho(K_f;p_2)S\left(k+\frac{q}{2}\right)\ \gamma^\mu\ S\left(k-\frac{q}{2}\right)$$
$$\times\Gamma_\pi(K_i;p_1)S\left(k-\frac{p_1+p_2}{2}\right)\Big\} + (e_{\bar{q}}\ \text{term})\ , \tag{2}$$

where $K_f = k - p_1/2$, $K_i = k - p_2/2$, $\Gamma_\pi(k;p)$ and $\Gamma^\nu_\rho(k;p)$ are the vertex functions of π and ρ mesons, $S(k)$ is the quark propagator, and e_q is the quark charge operator which takes on values of $e_u = \frac{2}{3}$ and $e_d = -\frac{1}{3}$. Our calculated form factor, shown in Fig. 3, falls off much more rapidly at large Q^2 than the monopole based on vector meson dominance (VMD) used by Hummel and Tjon; it is about a factor of 3 times smaller at $Q^2 = 200$ fm^{-2}. The calculated value of $g_{\rho\pi\gamma}$ is 0.71, in fair agreement with the recently measured value of 0.56 [17].

We now turn to a discussion of the $\omega\sigma\gamma$ exchange current. Here we are less able to present a reliable calculation, partly because it is unclear whether to take the "σ" to be the observed $I = 0$ resonance with a mass in the vicinity of 1000 MeV, or the phenomenological two pion enhancement which plays a role in all OBE models of the nuclear force and which has a mass in the vicinity of 500 MeV. In our estimate we will follow Ref. [11] and assume the latter. We also assume this sigma to be the chiral partner of the pion [18, 19], which suggests, in the spirit of the Nambu–Jona-Lasinio model [19], that the $\sigma q\bar{q}$ vertex can be obtained from the $\pi q\bar{q}$ vertex by replacing the factors of $\gamma^5\chi_f$ by the unit matrix (so that the momentum dependence is the same). Similarly, we will use the same parametrization for the $\omega q\bar{q}$ vertex as we did for the $\rho q\bar{q}$ vertex.

The calculation of the $\omega\sigma\gamma$ form factor from the quark loop diagram in Fig. 1(c) is complicated by the fact that this simple loop diagram is, by itself, not gauge invariant. To obtain a gauge invariant result we must take account of the interaction currents induced by the nonlocality of the meson-$q\bar{q}$ vertices. Given models of $\omega q\bar{q}$ and $\sigma q\bar{q}$ vertices, $\Gamma_\omega(k,p)$ and $\Gamma_\sigma(k,p)$, the method of minimal substitution [20] gives explicit forms for these interaction currents,

$$\mathcal{J}^\mu_{\sigma q\bar{q}}(k;p,q) = e_u\left[\Gamma_\sigma\left(k-\frac{q}{2},p\right) - \Gamma_\sigma(k,p)\right]\frac{[4k-q]^\mu}{q\cdot[4k-q]} + (e_{\bar{d}}\ \text{term}), \tag{3a}$$

$$\overline{\mathcal{J}}^\mu_{\omega q\bar{q}}(k;p,q) = e_u\,\epsilon_\nu\left[\overline{\Gamma}^\nu_\omega(k,p) - \overline{\Gamma}^\nu_\omega\left(k+\frac{q}{2},p\right)\right]\frac{[4k+q]^\mu}{q\cdot[4k+q]} + (e_{\bar{d}}\ \text{term}), \tag{3b}$$

where the $e_{\bar{d}}$ term is obtained by replacing $q \to -q$ in the e_u term. Adding these two contributions the quark loop diagram for the $\omega\sigma\gamma$ amplitude gives two independent, gauge invariant terms:

$$\langle\omega(p_2)|J^\mu|\sigma(p_1)\rangle = \mathcal{G}^{(a)}(Q^2)[(q\cdot p_1)\epsilon^\mu - (\epsilon\cdot q)p_1^\mu] + \mathcal{G}^{(b)}(Q^2)[(q\cdot p_2)\epsilon^\mu - (\epsilon\cdot q)p_2^\mu], \tag{4}$$

where $\mathcal{G}^{(a)}(Q^2)$ and $\mathcal{G}^{(b)}(Q^2)$ are independent functions of Q^2. These two terms also appear in models in which the sigma is treated as a composite two pion system [21].

Numerical evaluation shows that the two independent functions $\mathcal{G}^{(a)}(Q^2)$ and $\mathcal{G}^{(b)}(Q^2)$ have opposite sign and are nearly equal in magnitude (the sum of these two functions is less than 20% of their difference). In addition, the sum vanishes if $m_\omega \simeq m_\sigma$ and decreases more rapidly with Q^2 than the difference. For all of these reasons we approximate the $\omega\sigma\gamma$ vertex by

$$\langle\omega(p_2)|J^\mu|\sigma(p_1)\rangle = \frac{e}{m_\omega}g_{\omega\sigma\gamma}f_{\omega\sigma\gamma}(Q^2)[q^2\epsilon^\mu - (\epsilon\cdot q)q^\mu], \tag{5}$$

where $\frac{e}{m_\omega}g_{\omega\sigma\gamma}f_{\omega\sigma\gamma}(Q^2) = \mathcal{G}^{(a)}(Q^2) = -\mathcal{G}^{(b)}(Q^2)$. The coupling constant is defined by the normalization $f_{\omega\sigma\gamma}(0) = 1$. We emphasize that Eq. (5) is only an approximation to the full result given in Eq. (4), and that its tensor structure, $q^2\epsilon^\mu - (\epsilon\cdot q)q^\mu$, differs from $(q\cdot p_1)\epsilon^\mu - (\epsilon\cdot q)p_1^\mu$, the result conventionally used. However, the integral over the exchange current operator [Fig. 1(b)] is approximately symmetric under the replacement $p_1 \leftrightarrow -p_2$, and the two tensor forms are therefore approximately equivalent. Our numerical result for $f_{\omega\sigma\gamma}(Q^2)$ is shown in Fig. 3. Note that the factorization assumption, $f_{\omega\sigma\gamma}(Q^2) = \text{constant} \times f_{\rho\sigma\gamma}(Q^2)$, works approximately at large Q^2 ($Q^2 > 3$ GeV$^2/c^2$), as suggested by power counting. Factorization does not work at low Q^2, where the form factors are strongly affected by the difference in the matrix structure of the $\rho\pi\gamma$ and $\omega\sigma\gamma$ loops.

Figure 2(a) shows the effects of different models for $f_{\rho\pi\gamma}(Q^2)$ and $f_{\omega\sigma\gamma}(Q^2)$ on the deuteron structure function $A(Q^2)$. Because Hummel and Tjon used a VMD form factor (the dotted line in Fig. 3), their $\rho\pi\gamma$ exchange current was too large at high Q^2, and they needed

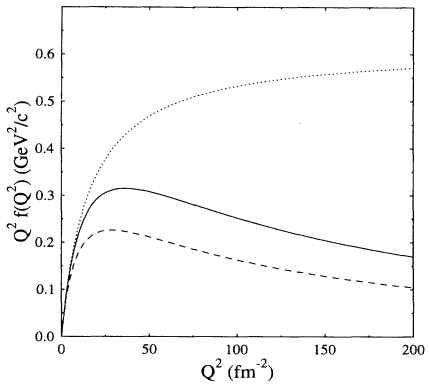

FIG. 3. The QL $\rho\pi\gamma$ (solid line) and $\omega\sigma\gamma$ (dashed line) form factors multiplied by Q^2. The VDM form factor (dotted line) is shown for comparison.

another exchange current to cancel it. The $\omega\sigma\gamma$ MEC has the opposite sign, and assuming factorization and $g_{\rho\pi\gamma} = -g_{\omega\sigma\gamma} = 0.56$ results in a strong cancellation of these MECs, as shown in Fig. 2(a) (the curve shown here is a corrected version of the original curve published in Ref. [11]). Using quark loop (QL) form factors, the $\omega\sigma\gamma$ MEC is very small, the cancellation is much less sensitive, and the $\rho\pi\gamma$ MEC current gives better agreement with the data.

Next, consider $B(Q^2)$ shown in Fig. 2(b). The $\rho\pi\gamma$ MEC makes only a small contribution to $B(Q^2)$, and Hummel and Tjon found that they could obtain agreement with the data [22] only by introducing the $\omega\sigma\gamma$ MEC. However, the position of the diffraction minimum is very sensitive to the choice of the $\omega\sigma\gamma$ form factor, and while good agreement was obtained with the VMD model, the more realistic QL model does not succeed in fitting the data.

In conclusion, we emphasize that the high Q^2 predictions for $A(Q^2)$ depend strongly on the $\rho\pi\gamma$ form factor. Our quark loop calculation may not be reliable enough to give a definitive result for this form factor, but does strongly suggest that it is probably much softer than the one obtained from the vector dominance model. $A(Q^2)$ is also sensitive to the (unknown) size of the neutron charge form factor (see Ref. [4]). Taking these considerations into account, we find that A could easily be explained by some combination of a $\rho\pi\gamma$ exchange current and an enhanced neutron charge form factor, but that, in the absence of measurements of the neutron charge form factor and a definitive calculation (or measurement) of the $\rho\pi\gamma$ form factor, it is difficult to fix this combination. The situation is different for B, where the contributions from *both* the $\rho\pi\gamma$ exchange current *and* the neutron charge form factor are negligible. Attempts to use an $\omega\sigma\gamma$ exchange current to explain B are not successful unless an unrealistically hard form factor is used. We conclude that the B form factor is not explained by these models.

The authors are deeply indebted to Professor John Tjon and Dr. E. Hummel for supplying their nuclear matrix elements of the $\rho\pi\gamma$ and $\omega\sigma\gamma$ current operators. H.I. acknowledges useful discussions with Professor S. J. Wallace, Dr. Neal Devine, and Professor Mark Strickman. The work of H.I. is partly supported by the Department of Energy Grant No. DE-FG05-86-ER40270 for the Center for Nuclear Studies, at the George Washington University. The work of F.G. is partly supported by DOE Grant No. DE-FG05-88ER40435.

[1] D. O. Riska and G. E. Brown, Phys. Lett. **38B**, 193 (1972); M. Bernheim *et al.*, Nucl. Phys. **A365**, 349 (1981).
[2] E. Nyman and D. O. Riska, Phys. Rev. Lett. **57**, 3007 (1986); Nucl. Phys. **A468**, 473 (1987); M. Wakamatsu and W. Weise, Nucl. Phys. **A477**, 559 (1988).
[3] M. Oka and K. Yazaki, Phys. Lett. **90B**, 41 (1980); S. Takeuchi and K. Yazaki, Nucl. Phys. **A438**, 605 (1985); Y. Yamauchi and M. Wakamatsu, Nucl. Phys. **A457**, 621 (1986); H. Ito and A. Faessler, Nucl. Phys. **A470**, 626 (1987); T. de Forest and P. J. Mulders, Phys. Rev. D **35**, 2849 (1987); H. Ito and L. S. Kisslinger, Phys. Rev. C **40**, 887 (1989); A. E. L. Dieperink and P. J. Mulders, Nucl. Phys. **A497**, 253c (1989).
[4] R. G. Arnold, C. Carlson, and F. Gross, Phys. Rev. C **21**, 1426 (1980).
[5] J. A. Tjon and M. J. Zuilhof, Phys. Lett. **84B**, 31 (1979); M. J. Zuilhof and J. A. Tjon, Phys. Rev. C **22**, 2369 (1980).
[6] R. Blankenbecler and R. Suger, Phys. Rev. **142**, 1051 (1966).
[7] P. L. Chung, F. Coester, B. D. Keister, and W. N. Polyzou, Phys. Rev. C **37**, 2000 (1988).
[8] L. L. Frankfurt, I. L. Grach, L. A. Kondratyuk, and M. I. Strickman, Phys. Rev. Lett. **62**, 387 (1989).
[9] F. Gross, J. W. Van Orden, and K. Holinde, Phys. Rev. C **45**, 2094 (1992).
[10] R. Machleidt, K. Holinde, and Ch. Elster, Phys. Rep. **149**, 1 (1987).
[11] E. Hummel and J. A. Tjon, Phys. Rev. Lett. **63**, 1788 (1989); Phys. Rev. C **42**, 423 (1990).
[12] R. J. Adler and S. D. Drell, Phys. Rev. Lett. **13**, 349 (1964).
[13] M. Chemtob, E. Moniz, and M. Rho, Phys. Rev. C **10**, 344 (1974).
[14] M. Gari and H. Hyuga, Nucl. Phys. **A264**, 409 (1976).
[15] H. Ito, W. Buck, and F. Gross, Phys. Rev. C **45**, 1918 (1992); **43**, 2483 (1991).
[16] H. Ito, W. Buck, and F. Gross, Phys. Lett. B **287**, 23 (1992).
[17] D. Berg *et al.*, Phys. Rev. Lett. **44**, 706 (1980).
[18] R. Delbourgo and M. D. Scadron, Phys. Rev. Lett. **48**, 379 (1982).
[19] Y. Nambu and G. Jona-Lasinio, Phys. Rev. **122**, 345 (1961).
[20] K. Ohta, Phys. Rev. C **40**, 1335 (1989).
[21] S. M. Berman and S. D. Drell, Phys. Rev. **133**, 791 (1964).
[22] R. G. Arnold *et al.*, Phys. Rev. Lett. **58**, 1723 (1987).